J|A|C|S ARTICLES

Published on Web 07/09/2009

Quantitative Evaluation of Metal−Molecule Contact Stability at the Single-Molecule Level

Makusu Tsutsui,[†] Masateru Taniguchi,*[,†,‡] and Tomoji Kawai*[,†]

The Institute of Scientific and Industrial Research, Osaka University, Ibaraki, Osaka 567-0047, Japan, and PRESTO, Japan Science and Technology Agency, Honcho, Kawaguchi, Saitama 332-0012, Japan

Received April 9, 2009; E-mail: taniguti@sanken.osaka-u.ac.jp

Abstract: Practical realization of any electronic device requires a quantitative measure of their durability for the sake of guaranteeing the reliability. Unfortunately, however, there exists no such tool for molecular devices. The present article provides a solution to this issue in molecular electronics by reporting an experimental demonstration of a quantitative comparison of thermodynamic stability of single-molecule junctions consisting of two distinct anchor groups: thiol and amine. We report solid evidence that Au−thiol bonds are far more stable than Au−amine linkages through exhibiting 2-fold longer natural lifetime of Au−aminobenzenethiol−Au single-molecule junctions compared to the Au−benzenediamine−Au counterpart. We also find that a single-molecule device composed of Au−thiol links is a factor of 100000 more stable than that configured with Au−amine contacts.

Introduction

There has been significant progress in exploring electron transport through an individual molecule connected to two electrodes.[1−3] Besides the fundamental understanding of electrical characteristics of metal−molecule−metal systems, an important step toward the practical realization of a single-molecule device is development of metal−molecule contacts with practical stability. From this perspective, it is important to deepen insight into the chemical nature of the metal−molecule link and establish guidelines for selecting optimal anchor groups. However, less effort has been devoted to this issue, and little is known about the electrical and thermal stability of metal−molecule−metal junctions.

First requisite for examining metal−molecule contact stability is a technique to fabricate molecular junctions. The mechanical break junction method is one of the few techniques that enable control of the number of molecules bridging a pair of electrodes.[4] In this method, a metal nanoconstriction is broken by mechanical stretching. After the junction breaking, two metal electrodes with a nanoscale gap in between are formed. Usually, a targeted molecule is adsorbed on the junction in advance, so as to have the molecules trapped in the nanogap and build metal−molecule−metal structures. When a few molecules are bridged between the electrodes, further electrode separation results in sequential breakdown of metal−molecule contacts. Eventually, a single-molecule junction is obtained right before the complete junction breakdown. Subsequently, in break junction experiments, the breaking process is reversed and a metal nanocontact is recreated. Repeating the open/close processes allows efficient fabrication of a number of single-molecule junctions with various metal−molecule configurations and molecular conformations, thereby providing an experimental platform for addressing electron transport properties of metal−molecule−metal junctions at the single-molecule level.[4−8]

Recently, the break junction method has also been applied for assessing metal−molecule contact stability.[9−16] The experimental concept follows the operational principle of single-molecule dynamic force spectroscopy, which is an important single-molecule technique widely applied for probing noncovalent molecular interactions in biological systems at the single-molecule level.[13,14,17] More specifically, in the experiments, the lifetime of a metal−molecule contact subjected to a mechanical stretching at a wide range of elongation speed v_d is measured. It has been demonstrated that the natural lifetime, i.e., the survival time of metal−molecule−metal junctions that fracture

[†] Osaka University.
[‡] Japan Science and Technology Agency.

(1) Tao, N. J. *Nat. Nanotechnol.* **2006**, *1*, 173.
(2) Galperin, M.; Ratner, M. A.; Nitzan, A.; Troisi, A. *Science* **2008**, *319*, 1056.
(3) Lindsay, S. M.; Ratner, M. A. *Adv. Mater.* **2008**, *19*, 23.
(4) Xu, B.; Tao, N. J. *Science* **2003**, *301*, 1221.
(5) Xiao, X.; Xu, B.; Tao, N. J. *Nano Lett.* **2004**, *4*, 267.
(6) Venkataraman, L.; Klare, J. E.; Nuckolls, C.; Hybertsen, M. S.; Steigerwald, M. L. *Nature* **2006**, *442*, 904.
(7) Wu, S.; Gonzalez, M. T.; Huber, R.; Grunder, S.; Mayor, M.; Schönenberger, C.; Calame, M. *Nat. Nanotechnol.* **2008**, *3*, 569.
(8) Liu, K.; Wang, X.; Wang, F. *ACS Nano* **2008**, *2*, 2315.
(9) Huang, Z.; Xu, B.; Chen, Y.; Di Ventra, M.; Tao, N. J. *Nano Lett.* **2006**, *6*, 1240.
(10) Huang, Z.; Chen, F.; Bennett, P. A.; Tao, N. J. *J. Am. Chem. Soc.* **2007**, *129*, 13225.
(11) Tsutsui, M.; Shoji, K.; Morimoto, K.; Taniguchi, M.; Kawai, T. *Appl. Phys. Lett.* **2008**, *92*, 223110.
(12) Tsutsui, M.; Taniguchi, M.; Kawai, T. *Nano Lett.* **2008**, *8*, 3293.
(13) Evans, E. *Faraday Discuss.* **1998**, *111*, 1.
(14) Markel, R.; Nassoy, P.; Leung, A.; Titchie, K.; Evans, E. *Nature* **1999**, *397*, 50.
(15) Huisman, E. H.; Trouwborst, M. L.; Bakker, F. L.; de Boer, B.; van Wees, B. J.; van der Molen, S. J. *Nano Lett.* **2008**, *8*, 3381.
(16) Kamenetska, M.; Koentopp, M.; Whalley, A. C.; Park, Y. S.; Steigerwald, M. L.; Nuckolls, C.; Hybertsen, M. S.; Venkataraman, L. *Phys. Rev. Lett.* **2009**, *102*, 126803.
(17) Evans, E.; Calderwood, D. A. *Science* **2007**, *316*, 1148.

10.1021/ja902871d CCC: $40.75

via thermal fluctuations under zero-force conditions, can be deduced by examining the junction stretching rate dependence of the contact lifetime.[10−12] Nevertheless, direct measurements of the natural lifetime are found formidable; difficulty lies in the fact that the junction lifetime is highly sensitive (exponentially dependent) to the force and even picometer-scale mechanical fluctuations can cause severe contact destabilizations, impeding accurate evaluations of the metal−molecule contact stability.[10,11] In order to overcome this technical barrier, we have previously developed "self-breaking technique".[11−13] It exploits the outstanding mechanical stability of nanofabricated mechanically controllable break junctions (MCBJs), which permits direct estimation of the natural lifetime of atomic and molecular junctions.[18,19] The present study reports a quantitative comparison of the thermodynamic stability of the two most widely studied metal−molecule systems, Au−S and Au−NH_2,[20−23] through systematic measurements of the contact natural lifetime using this self-breaking technique.

Experimental Section

The lithographically defined MCBJs were fabricated as follows.[18,19,24] A phosphorus bronze substrate (thickness ~ 0.5 mm) was coated with about a 4 μm thick polyimide layer for insulation. Subsequently, Au nanoscale junctions were patterned using standard electron beam lithography and radiofrequency magnetron sputtering processes. Finally, the polyimide underneath the junctions was removed via isotropic reactive ion etching to obtain free-standing Au nanojunctions. The sample configurations were designed to offer the displacement ratio $r = \Delta d/\Delta z \sim 2 \times 10^{-4}$, where Δd and Δz denote the displacements of the junctions and the moving distance of the pushing rod that bends the substrate, respectively.[24] Calibration measurements were performed for r by analyzing $I - \Delta d$ characteristics where I is the tunnel current flowing through a nanogap formed by breaking the junctions,[17,25−27] and the samples that showed r within 10% error have been employed. The experiments started by breaking the junctions in a dilute 1,2,4-trichlorobenzene solution of test molecules (~0.01 mM): aminobenzenethiol (ABT), or benzenediamine (BDA). 1,2,4-Trichlorobenzene was purchased from Sigma-Aldrich, and ABT and BDA molecules were purchased from Tokyo Chemical Industry. All the chemicals were used as received. These molecules were chosen in order to directly compare the stability of Au−S and Au−NH_2 linkages (Figure 1). More specifically, we have previously reported the thermodynamic stability of Au−S contacts through lifetime measurements of Au−benzenedithiol (BDT)−Au junctions.[11] Similarly, we expect that the stability of Au−NH_2 can be studied by measuring the lifetime of the BDA junctions consisting of two Au−NH_2 contacts. For ABT junctions, on the other hand, the molecule is anchored via Au−S and Au−NH_2. Thus, it is logically anticipated that the robustness of the two types of metal−molecule contacts can be directly compared by examining the difference in the natural lifetime between ABT and BDA (BDT). After the initial breakage, the sample chamber was evacuated. Then, we opened/closed the junctions repeatedly in a vacuum (~10^{-5} Torr) at room temperature under well-controlled junction stretching conditions using our resistance feedback program.[13] This allows reproducible formation of stable metal−molecule−metal junctions with a specific configuration.[11−13] Throughout the experiments, junction conductance was measured using a picoammeter (Keithley 6487) under a dc bias voltage of 0.2 V. Simultaneously, a digital oscilloscope (LeCroy WaveRunner 6050A) was utilized to monitor rapid junction breakdown, which records the potential drop at the current sensing resistor (10 kΩ) connected in series to the junction.

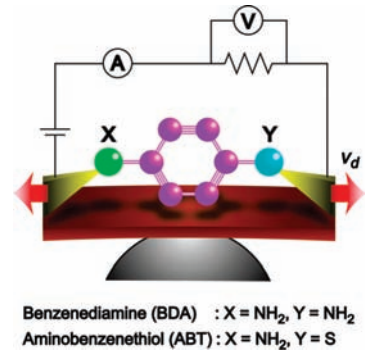

Figure 1. A schematic illustration of the break junction experiments using the nanofabricated mechanically controllable break junctions. The two nanoelectrodes are move in and out of contact to repeatedly form and break a single-molecule junction. In the experiments, junction stretching is implemented at a constant speed v_d, and concomitant temporal conductance change is recorded using a low dc bias voltage of 0.2 V.

Results and Discussion

Single-Molecule Conductance Measurements. The first step in evaluations of metal−molecule contact stability is to measure the single-molecule conductance of metal−molecule−metal junctions of concern.[11] We investigated the electron transport properties of ABT and BDA molecules by monitoring temporal changes in the electrical conductance during breaking of the junctions at $v_d = 6$ nm/s. The conductance measurements are exhibited for 2000 consecutive trials of the junction breaking. The initial stage of the break junction experiments involves mechanical elongation of Au−Au nanocontacts. Correspondingly, the junction conductance does not decrease smoothly but discretely upon gradual thinning of the nanoconstriction. When the conductance is diminished to around 1 G_0 ($G_0 = 2e^2/h$ is the conductance quantum, where e and h are the electron charge and Planck's constant, respectively), a long plateau is often observed. The 1 G_0 state is a characteristic feature of Au single-atom contacts that possess one transparent channel for electron transmission.[24] Further stretching leads to complete breakdown of the Au junctions and associated rapid conductance drops. In many cases (50−60% of 2000 conductance traces examined), the conductance simply drops to zero after the Au contact separation, which is indicative of electron tunneling through a vacuum gap between the two nanoelectrodes formed. The other traces (30−40%) demonstrate conductance steps at around 0.01 G_0 for both BDA and ABT after the single-atom contact breakdown, as presented in Figure 2a. Occurrence rates of the characteristic low-conductance steps are summarized in Figure 2b. The rest of the curves (less than 10%) showed a rather smooth decrease of conductance to zero without showing any step-like features. Histograms constructed with the data displaying steps in the low-conductance regime reveal multiple peak

(18) Tsutsui, M.; Shoji, K.; Taniguchi, M.; Kawai, T. *Nano Lett.* **2008**, *8*, 345.
(19) van Ruitenbeek, J. M.; Alvarez, A.; Pineyro, I.; Grahmann, C.; Joyez, P.; Devoret, M. H.; Esteve, D.; Urbina, C. *Rev. Sci. Instrum.* **1996**, *67*, 108.
(20) Chen, F.; Li, X.; Hihath, J.; Huang, Z.; Tao, N. J. *J. Am. Chem. Soc.* **2006**, *128*, 15874.
(21) Venkataraman, L.; Klare, J. E.; Tam, I. W.; Nuckolls, C.; Hybertsen, M. S.; Steigerwald, M. L. *Nano Lett.* **2006**, *6*, 458.
(22) Quek, S. Y.; Venkataraman, L.; Choi, H. J.; Louie, S. G.; Hybertsen, M. S.; Neaton, J. B. *Nano Lett.* **2007**, *7*, 3477.
(23) Prodan, E.; Car, R. *Nano Lett.* **2008**, *8*, 1771.
(24) Agraït, N.; Yeyati, A. L.; van Ruitenbeek, J. M. *Phys. Rep.* **2003**, *377*, 81.
(25) Vrouwe, S. A. G.; van der Giessen, E.; van der Molen, S. J.; Trouwborst, M. L.; van Wees, B. J. *Phys. Rev. B* **2005**, *71*, 035313.
(26) Lörtscher, E.; Weber, H. B.; Riel, H. *Phys. Rev. Lett.* **2007**, *98*, 176807.
(27) Tsutsui, M.; Taniguchi, M.; Kawai, T. *Appl. Phys. Lett.* **2008**, *93*, 163115.

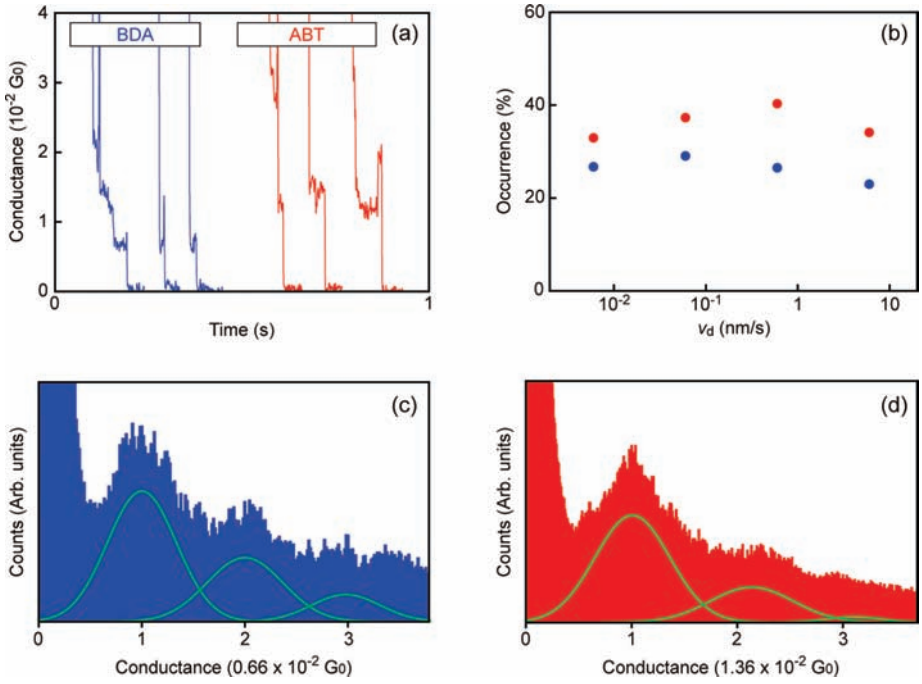

Figure 2. (a) An example of the conductance curves obtained for BDA (blue) and ABT (red) junctions at $v_d = 6$ nm/s. (b) Occurrence rates of conductance steps at ~ 0.01 G_0 for BDA (blue) and ABT (red) plotted as a function of v_d. (c) Conductance histograms of BDA and (d) ABT junctions built with the conductance curves that demonstrate clear step structures at the low-conductance regime. The bin size is 10^{-4} G_0. The green lines are the Gaussian fit. Multiple peaks regularly positioned with a constant interval of $G_{BDA} = 0.0066$ G_0 and $G_{ABT} = 0.0136$ G_0 denote characteristic conductance states of BDA and ABT junctions, respectively, with the peaks at 1 $G_{BDA(ABT)}$, 2 $G_{BDA(ABT)}$, and 3 $G_{BDA(ABT)}$ representing molecular transport junctions constructed with one, two, and three molecules bridging the electrodes in parallel.

profiles (Figure 2c,d). The peaks are regularly spaced with a constant interval of about 0.0066 G_0 and 0.0136 G_0 for BDA and ABT junctions, respectively. Such distinct peak structures are never observed in cases where no molecules are introduced. The low-conductance peaks are, therefore, attributable to electron transport in the metal−molecule−metal junctions with their positions denoting the number of molecules trapped in the electrode nanogaps.[4] From this result, single-molecule conductance of $G_{BDA} = 0.0066$ G_0 and $G_{ABT} = 0.0136$ G_0 is obtained for BDA and ABT molecules, respectively (It is worth noting that G_{BDA} is in good agreement with that reported by Venkataraman et al.[21,22]).

What makes G_{ABT} higher than G_{BDA}? In the electron transport through metal−molecule−metal structures, the energy alignment at the metal−molecule interface plays a crucial role on the electron transmissivity. We performed density functional theory calculations using GAUSSIAN03[28] with B3LYP functional and 6-31G** basis set for the HOMO−LUMO gaps ΔE of the two molecules and obtained $\Delta E_{BDA} = 6.35$ eV and $\Delta E_{ABT} = 5.60$ eV for BDA and ABT, respectively. The smaller ΔE of ABT molecules indicates lower carrier injection barrier at the metal−molecule contacts and hence accounts for the higher conductivity of the ABT junctions in comparison to the BDA counterpart.

The conductance measurements are extended to low-v_d conditions down to $v_d = 0.006$ nm/s. G_{BDA} and G_{ABT} are plotted as a function of v_d in Figure 3. Error bars denote the full width at half-maximum of the single-molecule peaks, $\Delta G_{BDA(ABT)}$. As shown in Figure 3, G_{BDA} and G_{ABT} remain almost constant in the v_d range measured. In contrast, ΔG_{BDA} is relatively small compared to ΔG_{ABT}, which indicates wider distributions of

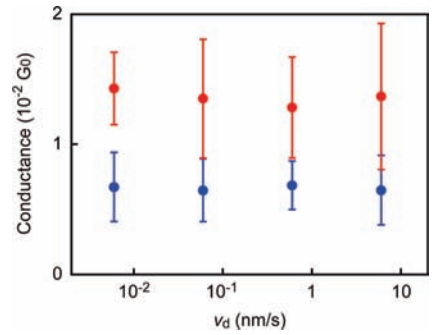

Figure 3. Plots of G_{BDA} (blue) and G_{ABT} (red) as a function of v_d. The error bars are the full width at half-maximum of the corresponding single-molecule conductance peaks. The comparatively larger conductance variations of ABT junctions in comparison to the BDA counterpart reflect the more extensive metal−contact configuration diversity at the Au−S link compared to that of Au−NH_2.

single-molecule conductance for ABT than BDA. The experimental junction to junction variance of single-molecule conductance is usually attributed to molecular conformations and metal−molecule contact configurations.[5,29−31] We expect little difference in the conformational nature of the center benzene ring for the two molecules.[6] Thus, the fact that $\Delta G_{BDA} < \Delta G_{ABT}$ is ascribed to roles of the anchor groups on electron transport. It has been well studied that conductance of dithiol molecules varies extensively for more than 1 order of magnitude depending on the Au−S configurations.[29,30] In contrast, diamine linkers are found to yield more specific single-molecule conductance

(28) Frisch, M. J. et al. *Gaussian03, revisionC.02*; Gausian, Inc., Pittsburgh, PA, 2003.

(29) Li, X.; He, J.; Hihath, J.; Xu, B.; Lindsay, S. M.; Tao, N. J. *J. Am. Chem. Soc.* **2006**, *128*, 2135.
(30) Basch, H.; Cohen, R.; Ratner, M. A. *Nano Lett.* **2005**, *5*, 1668.
(31) González, M. T.; Wu, S.; Huber, R.; van der Molen, S. J.; Schönenberger, C.; Calame, M. *Nano Lett.* **2006**, *6*, 2238.

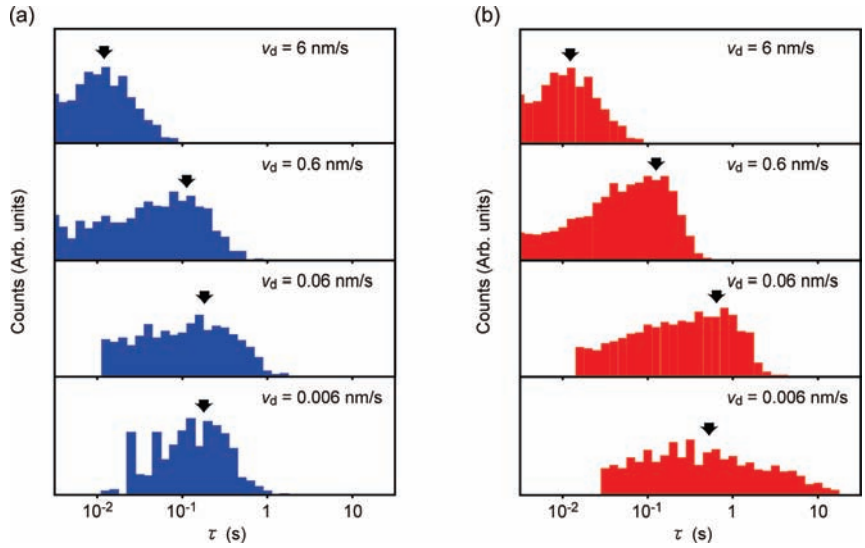

Figure 4. τ histograms of (a) BDA and (b) ABT junctions at various v_d conditions. Logarithmic bins are used. Each histogram consists of traces that showed characteristic steps near the single-molecule conductance. The arrows indicate the single peak position, the lifetime τ_B of which corresponds to the lifetime of single-molecule junctions of a specific configuration.

by virtue of restricted binding sites for amines on the Au surface that provides well-defined metal−molecule contact configurations.[20−22] The larger variation in G_{ABT} can be, therefore, interpreted as stemming from relatively diverse metal−molecule bond geometries involved at the Au−S link.

It is worth noting that occurrence of the low conductance steps presented in Figure 2b are lower for BDA than ABT over the v_d range measured. The less frequent formation of BDA junctions can be explained qualitatively by considering expected weaker Au−NH_2 bonds compared to Au−S links.[20,32] Unlike measurements carried out in a liquid environment, there is no way for molecules to be supplied into the junction nanogap in a vacuum. Therefore, it is preferred for molecules to be adsorbed tightly on surface for forming metal−molecule−metal junctions, since otherwise weakly bonded molecules would be more feasibly removed from the contact region during junction-closing processes. This can be a possible explanation for the observed higher chance of metal−molecule−metal junction formations for ABT, which is strongly connected on the junctions via Au−S linkage.

Stretching Rate Dependence of a Single Molecule Junction Lifetime. In addition to the electron transport characteristics, the conductance measurements also provide information concerning the stability of the molecular junctions.[11] As explained above, the plateaus that emerge at G_{BDA} (or G_{ABT}) signify formation of single-molecule junctions. The plateau length in turn represents the junction lifetime τ. Theoretically, τ of a single-molecule junction subjected to a mechanical stretching force F and a bias voltage of 0.2 V is described by the Arrhenius-type expression as

$$\tau = \left(\frac{1}{f_0}\right)\exp\left(\frac{E_B - \chi_\beta F}{k_B T_0}\right) \quad (1)$$

where f_0, E_B, χ_β, and T_0 denote the attempt frequency, the energy barrier against the junction breakdown, the thermally averaged projection of the displacements along the reaction coordinate of the molecular junctions to the actual elongation direction, and the ambient temperature, respectively.[33,34] This reflects the nature of the molecular junctions that undergo thermoactivated spontaneous breakdown.[10−12] The high-field phenomena such as current-induced forces and local heating are not included in eq 1, because their effects on τ are negligible at 0.2 V.[12,33,35−38] Under high v_d conditions, it is anticipated that tensile force accumulated at the metal−molecule contacts plays a significant role on the breakdown characteristics.[11] The aim of this work is to directly compare the room temperature stability of Au−S and Au−NH_2 linkages. For this purpose, we need to determine the natural lifetime of the metal−molecule contacts, i.e., τ at $F = 0$ N.

We find in the conductance curves that lowering v_d tends to prolong τ, which suggests non-negligible role of F on τ. The v_d dependence is investigated in detail by analyzing the statistical distributions of τ. A conductance window to extract τ from each conductance curve was defined as $G = G_{BDA(ABT)} \pm (\Delta G_{BDA(ABT)}/2)$. τ is acquired from each conductance curve by counting all the data points within the conductance window. The thus-built τ histograms are presented in Figure 4. Logarithmic bins are used instead of linear bins so as to represent junction-to-junction variations of E_B by the τ distributions, since τ is an exponential function of E_B as shown by eq 1. It should first be noted that τ spreads expansively for more than 4 orders of magnitude. This is naturally ascribed to a variation in metal−molecule contact configurations and/or molecular conformations of the single-molecule junctions fabricated in the experiments that generates E_B distributions.[11,12] Another important aspect is that the histograms represent a single peak structure, manifesting a single peak profile in E_B distributions as well and hence a preferred formation of the single-molecule junctions of a specific

(32) Park, Y. S.; Whalley, A. C.; Kamenetska, M.; Steigerwald, M. L.; Hybertsen, M. S.; Nuckolls, C.; Venkataraman, L. *J. Am. Chem. Soc.* **2007**, *129*, 15768.
(33) Todorov, T. N.; Hoekstra, J.; Sutton, A. P. *Phys. Rev. Lett.* **2001**, *86*, 3606.
(34) Evans, E. *Annu. Rev. Biophys. Biomol. Struct.* **2001**, *30*, 105.
(35) Di Ventra, M.; Chen, Y.-C.; Zwolak, M. *Nano Lett.* **2003**, *3*, 1691.
(36) Huang, Z.; Chen, F.; D'Agosta, R.; Bennett, P. A.; Di Ventra, M.; Tao, N. J. *Nat. Nanotechnol.* **2007**, *2*, 698.
(37) Di Ventra, M.; Pentelides, S. T.; Lang, N. D. *Phys. Rev. Lett.* **2002**, *88*, 046801.
(38) Yang, Z.; Chshiev, M.; Zwolak, M.; Chen, Y.-C.; Di Ventra, M. *Phys. Rev. B* **2005**, *71*, 041402.

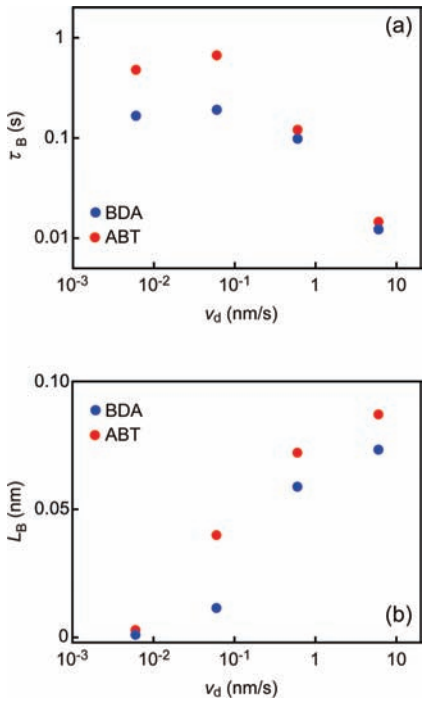

Figure 5. (a) Plots of τ_B and (b) L_B with respect to v_d.

configuration.[11,12,18] It is evident from Figure 4 that τ become longer with decreasing v_d. For quantitative analysis of the $\tau-v_d$ relation, we extracted the peak lifetime τ_B from each histogram. The stretching rate dependence is now clearly visualized by the τ_B-v_d plots in Figure 5a. The elongation length $L_B = v_d\tau_B$ at which the junction fractures is also displayed in Figure 5b as a function of v_d.[10,11] As shown by the data, L_B scales linearly with $\log(v_d)$ at $v_d > 0.06$ nm/s, which is a sign of force-accelerated thermal breakdown of single-molecule junctions at $F > 0$ N as predicted by the thermodynamic bond breaking theory by Evans.[9,11,34] In contrast, further decreasing v_d to 0.006 nm/s leads L_B to approach zero. At the same time, τ_B no longer changes at $v_d \leq 0.06$ nm/s whereas it monotonically decreases with v_d at $v_d > 0.06$ nm/s. These results suggest self-breaking of the single-molecule junctions by thermal fluctuations under negligible F at $v_d \leq 0.06$ nm/s.[11,12,18] We can directly obtain the natural lifetime from τ_B in the self-breaking regime, which is $\tau_{BDA} \sim 0.2$ s and $\tau_{ABT} \sim 0.5$ s for BDA and ABT junctions. This means that BDA and ABT junctions can be held on average for less than 1 s at maximum because of the limit in τ posed by the thermal fluctuations at room temperature.

Quantitative Comparison of Au−S and Au−NH_2 Contact Stability. We now discuss quantitative difference of metal−molecule contact stability between Au−S and Au−NH_2. It is well-established that dithiol molecular junctions fracture at Au−Au bonds at the rear of strong Au−S linkages, attributed to the higher Au−S bond strength (~1.6 eV) compared to the Au−Au counterpart (~1.0 eV).[9−11,39] The thermal limit of the Au−S contact derived single-molecule junction lifetime of Au−BDT−Au system at room temperatures was found to be $\tau_{BDT} \sim 50000$ s in our previous work.[11] This lifetime is 5 orders of magnitude longer than τ_{ABT}. Thus, it is unlikely that Au−ABT−Au junctions break at Au−S sides of the contacts. The remaining possibility is that ABT is more prone to fracture at the Au−NH_2 bonds. We note that τ_{ABT} and τ_{BDA} agree within 1 order of magnitude. For BDA junctions, there is only the choice to break at one of the two Au−NH_2 linkages. The fact that ABT and BDA junctions share the similar stability strongly indicates that breakdown occurs at Au−NH_2 links of ABT junctions with their Au−S contacts being almost unaffected.

Furthermore, back calculations of E_B from eq 1 with $F = 0$ N yield $E_B \sim 0.69$ and 0.71 eV for BDA and ABT junctions, respectively. Here, it should be pointed out that this E_B of BDA is in excellent accordance with the theoretical bond strength recently reported.[19,40] These values are about 0.3 eV lower than that obtained for BDT junctions, reflecting the relatively weak Au−NH_2 coordinate bonds.[11] As a consequence, it is concluded that Au−NH_2 contacts provide relatively lower thermal stability that brings about 5 orders of magnitude difference in the room temperature stability when employed in metal−molecule−metal junctions compared to Au−S contacts.

It should be pointed out that the natural lifetime of BDA and ABT junctions is 1 order of magnitude shorter than that of Au single-atom contacts, $\tau_{Au} \sim 10$ s.[18] Thus, unlike the Au−Au contact rupture modes in BDT junctions, amine-anchored junctions are likely to dissociate spontaneously via thermal fluctuations at relatively weak Au−NH_2 coordinate bond, in consistent with the recent theoretical prediction.[41]

It remains unclear why there exits about 2-fold difference between τ_{BDA} and τ_{ABT} if both junctions fracture at the Au−NH_2 contacts. As a possible explanation, we notice that there are two amine anchoring groups in BDA while there is only one in ABT. When denoting the natural lifetime of a Au−NH_2 bond as τ_{Au-NH2}, it can be anticipated that $1/\tau_{BDA} = 2/\tau_{Au-NH2}$ under an assumption that the two metal−molecule contacts are identical and the thermal breakdown occur mutually independently. In case of ABT junctions, on the other hand, one side of the molecules is contacted to the electrodes via the robust Au−S linkage with the lifetime τ_{Au-S}. Therefore, the junction dissociation rate is depicted as $1/\tau_{ABT} = (1/\tau_{Au-NH2} + 1/\tau_{Au-S}) \cong 1/\tau_{Au-NH2}$ since $\tau_{Au-S} \gg \tau_{Au-NH2}$ as we have clarified in the preceding paragraph. This simple argument predicts that $\tau_{ABT} \cong 2\tau_{BDA}$, which plausibly explains the observed quantitative disagreement between τ_{ABT} and τ_{BDA}.

Conclusion

In summary, the room temperature stability of Au−S and Au−NH_2 contacts was directly compared by measuring the natural lifetime of BDA and ABT single-molecule junctions using the self-breaking technique. The junction lifetime demonstrated monotonic decline with decreasing v_d in the range of 6 nm/s $\geq v_d \geq$ 0.06 nm/s, while it turned out to level off at lower v_d. The natural lifetime of ABT single-molecule junctions deduced from the lifetime data in the self-breaking regime was 5 orders of magnitude shorter than that of BDT junctions. On the other hand, the room temperature durability of ABT junctions was similar to that of BDA junctions. The results unambiguously reveal that ABT junctions fracture at relatively weak Au−NH_2 link rather than at Au−S side of the contacts.

Supporting Information Available: Complete author list of ref 28. This material is available free of charge via the Internet at http://pubs.acs.org.

JA902871D

(39) Xu, B.; Xiao, X.; Tao, N. J. *J. Am. Chem. Soc.* **2003**, *125*, 16164.
(40) Michoff, M. E. Z.; Vélez, P.; Leiva, E. P. M. *J. Phys. Chem. C* **2009**, *113*, 3850.
(41) Li, Z.; Kosov, D. S. *Phys. Rev. B* **2007**, *76*, 035415.